

Enhanced Eosin Mineralization in Presence of Au(III) Ions in Aqueous Solutions Containing TiO₂ as Suspension

G.R. Dey* and P. Singh

Radiation & Photochemistry Division, Bhabha Atomic Research Centre, Trombay, Mumbai 400085, India

Abstract: Photo-catalytic mineralization of eosin in aerated 0.1% (w/v) TiO₂ suspended aqueous systems with and without Au³⁺ using 350 nm photo light was carried out. Eosin mineralization rate was significantly faster in 2×10⁻⁴ M Au³⁺ containing systems in contrast to sole TiO₂ systems, which is due to the participation of Au³⁺ and its in situ generated various reduced intermediates including gold nanoparticles during mineralization. Furthermore, pulse radiolysis (a well known transient measurement technique) was adopted to analyze the reaction intermediates (eosin-OH adducts and/or eosin radical cation) produced in mineralization by generating in situ ·OH and N₃ species. The reaction rates for ·OH and N₃ reactions with eosin evaluated respectively 5.4×10⁹ and 3.0×10⁹ dm³ mol⁻¹ s⁻¹ for the formation of radical cations were slower than the eosin-OH adduct formation rate (reaction rate = 1.4×10¹⁰ dm³ mol⁻¹ s⁻¹). Furthermore, it is proposed that the initially generated eosin-OH/hole adduct is undergoing mineralization in the presence of air/oxygen.

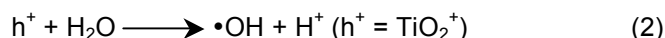
Keywords: TiO₂, Photolysis, Au(III) ions, Eosin, Gold nanoparticles, Mineralization.

1. INTRODUCTION

Color removal from industrial effluent is one of the most difficult requirements faced by the textile, dye manufacturing and paper industries. These industries are major consumers of water and, therefore cause water pollution; afterward it spreads to air and soil pollutions. Most of the dyes are harmful when brought in contact with living tissues. The discharge of such dyes into the river stream without proper treatment causes irretrievable damage to the crops and living beings, both aquatic and terrestrial. Some of them are not only toxic but also non biodegradable; hence they are not easily removed that is why there is an urgent need to develop effective methodology either by transforming them into harmless compounds or by mineralizing them completely. Mineralization of eosin, a model dye chosen under the study is generally used in cosmetics and biological stain for studying cell structures. Its soluble salts are normally used as dyes. Eosin has also been utilized as a groundwater migration tracer by capillary electrophoresis/laser-induced fluorescence employing a multi wavelengths laser. Eosin is a carcinogen [1], it causes also cheilitis, dermatitis and stomatitis and emits toxic fumes when heated [2].

Photo-catalytic technique for mineralization of organics using TiO₂ is recognized as an easiest and affordable process. On photo-irradiation (if the incident

photon energy $E_{hv} > E_{bg} \sim 3$ eV (band gap energy)) [3, 4], TiO₂ produces an electron (e⁻) - hole (h⁺) pair (charge carrier). The formation of hydroxyl radical (·OH) ($E^0 = 2.72$ V) [5, 6], a strong oxidant through TiO₂ photo-catalytic reactions as given below [3].



In presence of air/oxygen,



In the presence of an ·OH/h⁺ scavenger, it is possible to utilize TiO₂ containing aqueous systems as photo-reduction processes; otherwise, this system can be used as oxidation conditions by scavenging the photo-generated e⁻ (a strong reductant), most commonly with oxygen.

The mineralization of eosin is known wherein researchers have used TiO₂ based photo-catalysts [7-10] and the degradation rates reported therein through its absorption measurements, which were rather slow. In the present study, we have carried out the photo-catalytic mineralization of eosin using photosensitive semiconductor TiO₂ powder as suspension in water in presence of air/O₂. This work was explored further in presence of Au³⁺ (a probable electron scavenger) to check better/different mineralization kinetics subsists if any, which was the motivation of the work. The enhanced mineralization in Au³⁺ containing systems observed is reported in this article.

*Correspondence Address to this author at the Radiation & Photochemistry Division, Bhabha Atomic Research Centre, Trombay, Mumbai 400085, India; Tel: 91-22-2559 5397, 91-22-25595097; E-mail: grdey@barc.gov.in

P. Singh: project trainee from Sri Guru Granth Sahib World University, Fatehgarh Sahib, Punjab 140406, India.

2. MATERIALS AND METHOD

2.1. Chemicals

TiO₂ (Titanium(IV) oxide, -325 mesh, >99% purity having ~5% rutile) from Aldrich, Gold(III) chloride as HAuCl₄ (99.9% purity) from Fluka, India, eosin (>99% purity) from K&K Laboratories, New York, potassium permanganate, oxalic acid and sulphuric acid of AnalaR grades available in the laboratory were used without further purification.

Water from Millipore gradient A10 polishing system, with conductivity ~18.2 MΩ cm⁻¹ and organic carbon content < 5 ppb was used for all solutions preparations.

2.2. Photolysis and Evaluation

A quartz cell of 40 mL capacity was used for photo-irradiation with 350 nm light using Rayonet photo reactor having photon flux 4×10^{15} photons cm⁻² s⁻¹. The amount of solution used in photolysis experiments was 35 mL. The aerated (10 min air purged) aqueous solutions containing 0.1% (w/v) TiO₂ as suspension and 2×10^{-4} M eosin were photo-irradiated with constant stirring for different time at room temperature and normal atmospheric pressure. The total organic carbon (TOC) content was estimated adopting KMnO₄ demand method (well-known method for the determination of TOC contents). In brief, under this method we reflux a known but fixed amount of organic compound (eosin in this case) with known and standard KMnO₄ (5 mL of 0.001 M) in sulphuric acid (2 mL of 5 N) medium. The resulting solution was mixed with excess amount of standard oxalic acid (7 mL of 0.001 M). Later by doing volumetric analysis of the resulting mixture solution with standard KMnO₄, the amount of KMnO₄ required by the organic sample was estimated. The final amount of KMnO₄ demand with respect to TOC was evaluated by comparing KMnO₄ required in blank (sample without eosin) experiment. For consistency and reliability, under each set of experiments, the eosin mineralization curves were generated 3 to 5 times in KMnO₄ demand method as well as in spectrophotometric analyses, and the measurements errors remain < 10%.

2.3. Material Characterization

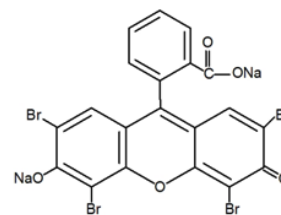
Membrane filters (Ultipor[®]N₆₆ Nylon 6.6 membrane 0.45 μm from PALL Life Sciences) were used for filtration under vacuum to separate TiO₂ from aqueous TiO₂ suspended systems when required. Characterizations of the photo-irradiated solutions and filtrates were done with a spectrophotometer (JASCO

V-650) and Dynamic light scattering (DLS), whereas the residues on membrane filters were characterized with different analytical techniques such as X-ray Diffractometer (XRD), Raman spectroscopy, Scanning Electron Microscopy (SEM) and Transmission Electron Microscopy (TEM).

Under DLS (Malvern Instruments Ltd, UK) studies, the gold nanoparticles (AuNP) over TiO₂ generated in photolysis were found highly poly-disperse in nature with average particle size of 100 nm. X-ray diffraction (XRD) measurement was carried out with Philips diffractometer (X'Pert PRO, PANalytical, Netherland) using Ni filtered Cu K_α radiation of 1.54 Å⁰ (~8 keV energy). XRD patterns of unknown samples were generally confirmed from the comparison of available data in literature and/or in library available in the software. Raman spectra were recorded at room temperature within the spectral range of 200-1800 cm⁻¹ using the 633 nm line from a HeNe laser with a charge-coupled device (CCD) (Synapse, Horiba Jobin Yvon) based monochromator (LabRAM HR800, Horiba Jobin Yvon, France). The data presented herein are free from the background interference. Furthermore, morphological characterization/images of the materials were obtained with JEOL JSM-T330 Scanning Electron Microscope (SEM) and Carl Zeiss LIBRA 120 kV (for TEM).

3. RESULTS AND DISCUSSIONS

Eosin (C₂₀H₆Br₄O₅Na₂), a red fluorescent dye possesses chemical structure as shown in Scheme 1. The mineralization of eosin under the study along with the morphological characterization of in situ generated materials is discussed below:



Scheme 1: Chemical structure of Eosin.

3.1. Photolysis of Eosin

The aerated 5×10^{-5} M eosin in aqueous solution was photo-irradiated at 350 nm light using above-mentioned photo reactor up to 120 min. 5 mL of photo-irradiated solutions were taken out at different time intervals and the UV-Vis absorption spectra recorded are shown in Figure 1a. The spectrum recorded for

eosin in aqueous solution prior to photolysis exhibits four peaks with absorption maxima at 255, 300, 340 and 516 nm (Figure 1a spectrum 'a'). The peak at 516 nm possesses high absorption intensity, which is the prime reason for taking low concentration of eosin for this particular experiment. With respect to photo-irradiation time, the absorbance at 516 nm was reduced as shown in the inset figure. This change is rather low indicating the photo-degradation/photo-decoloration of eosin was less under this condition. It is important to note that in this particular study the mineralization (transformation of eosin into CO₂ and water) should be negligible (discussed in the later section). Moreover, the decrease in absorbance at 516 nm is possibly due to the breaking of some of the weak chromophoric bonds of eosin molecule. This leads to ~20% of original color fading in 120 min photolysis. Furthermore, at other peaks positions (255, 300 and 340 nm), the changes in absorbance due to photolysis were quite low, hence are not considered for analysis.

3.2. Photolysis of Eosin in Presence of TiO₂

Similarly, photo-mineralization experiments were carried out in aerated 2×10⁻⁴ M eosin solutions in water containing 0.1% TiO₂ as suspension using 350 nm photolight up to 120 min with constant stirring conditions. The preference of 0.1% w/v TiO₂ in the present study was confirmed earlier for requisite TiO₂ amount for maximum photo-catalytic product yield [11]. The 5 mL photo-irradiated samples were taken out at

different time intervals and filtered using membrane filter and recorded absorption spectra of the filtrate solutions. The spectra recorded (not shown) exhibit abnormal behavior due to adsorption of eosin onto TiO₂, therefore we have tried to separate TiO₂ by centrifugal method (another separation technique) and the absorption spectra of the superannuated solutions were also recorded. In this method too it was difficult to measure eosin accurately; as a part of eosin adsorbed on TiO₂, moreover, the report on eosin adsorption in such system is available elsewhere [12]. Eventually, KMnO₄ demand method (discussed above) was adopted to estimate TOC content in eosin containing samples under different experimental conditions. The mineralization of eosin in TiO₂ containing systems interprets the decrease in TOC percentage (curve c) with respect to photolysis time as observed is shown in Figure 1b. The mineralization trend observed was relatively faster as compared to the mineralization of eosin without TiO₂ (inset of Figure 1a, which was generated using 5×10⁻⁵ M eosin) and without photolysis of the same system (curve b Figure 1b). The curve 'a' in Figure 1b generated in 2×10⁻⁴ M eosin photolysis using KMnO₄ demand was much slower than the absorbance change shown in Figure 1a inset, revealing the photolytic change of eosin without TiO₂ was due to photo-fading and not because of photo-mineralization. The mineralization rate of eosin evaluated (based on TOC measurement) from the plot of ln(C_t-C_∞)-lnC_∞ vs. photolysis time using the curve 'c' of Figure 1b was

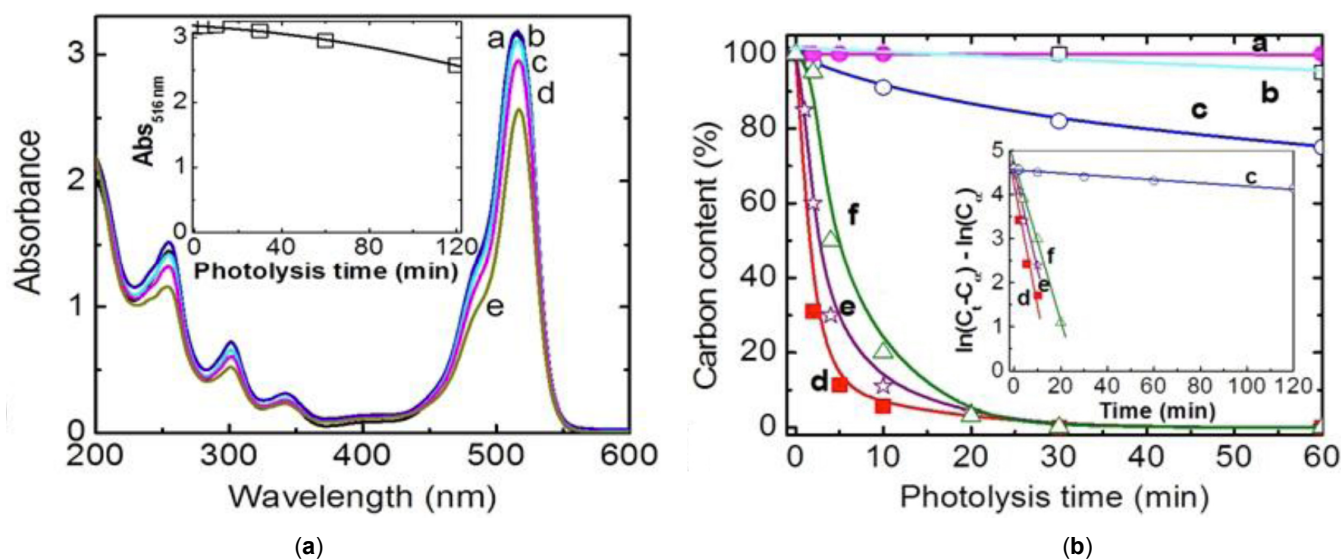


Figure 1: (a) The absorption spectra recorded for samples a: before and after b: 10; c: 30; d: 60 and e: 120 min photolysis of aerated 5×10⁻⁵ M eosin in aqueous solutions. Inset: the change in absorbance at 516 nm with respect to photolysis time. (b) Plots of total organic carbon contents (%) as determined by KMnO₄ demand method vs. photolysis time in a: only 2×10⁻⁴ M eosin; b: no photolysis 0.1% (w/v) TiO₂, 2×10⁻⁴ M eosin and 2×10⁻⁴ M Au³⁺; c: 0.1% (w/v) TiO₂ and 2×10⁻⁴ M eosin; d: 0.1% (w/v) TiO₂, 2×10⁻⁴ M eosin and 2×10⁻⁴ M Au³⁺; e: 0.1% (w/v) TiO₂, 2×10⁻⁴ M eosin and 5×10⁻⁵ M Au³⁺; f: 0.1% (w/v) TiO₂, 2×10⁻⁴ M eosin and 2×10⁻⁵ M Au³⁺ containing systems. Inset: plots of ln(C_t-C_∞)-lnC_∞ vs. time obtained for c-f mineralization curves

0.004 min^{-1} . Where C_t and C_∞ represent TOC contents respectively at time t and time ∞ (time ∞ represents the time where the TOC content becomes minimum/zero).

3.3. Photolysis of Eosin in Presence of TiO_2 and Au^{3+}

Photo-mineralization work was explored further to check the affect of Au^{3+} on eosin mineralization. For which aerated $2 \times 10^{-4} \text{ M}$ eosin in aqueous solution containing 0.1% (w/v) TiO_2 as suspension in presence of $2 \times 10^{-4} \text{ M}$ Au^{3+} were photo-irradiated under identical conditions. The absorption spectra of the superannuated solutions of the photo-irradiated solutions possess an absorption band around 516 nm (Figure 2a), which is due to the absorption of eosin (<2 min) for the initial experimental solutions and later (>5 min photolysis) due to AuNP formation revealing the active interference of AuNP in eosin analysis at $\lambda = 516 \text{ nm}$. To overcome the eosin analysis problem through absorption measurement, KMnO_4 demand method (discussed above) was adopted to determine the TOC contents. The results obtained are shown in Figure 1b curve d. The mineralization rate (0.274 min^{-1}) in this system was much faster (curve d) as compared to the systems of without Au^{3+} (curves a & c in Figure 1b). Similar experiments were also carried out with two different concentrations of Au^{3+} (2×10^{-5} and $5 \times 10^{-5} \text{ M}$) otherwise at identical conditions and the mineralization curves (curves e & f) generated are also shown in Figure 1b. The curves d-f in Figure 1b reveal that the mineralization kinetics of eosin depends on Au^{3+}

concentrations and the rates obtained were 0.224 and 0.180 min^{-1} respectively for 5×10^{-5} and $2 \times 10^{-5} \text{ M}$ Au^{3+} . It is noteworthy to include that bromide ion (Br^-) was identified qualitatively after separating TiO_2 in photo-mineralized eosin containing TiO_2 suspended aqueous systems both in presence and absence of Au^{3+} . The filtrate of mineralized samples changed the aqueous AgNO_3 solution to light yellow precipitate. It will also be useful to note here that the mineralization of eosin with pre-generated AuNP in TiO_2 containing systems was quite similar to Au^{3+} based systems under identical conditions.

3.4. Characterization of *In Situ* Generated Materials

As mentioned above, the photo-catalytic mineralization of eosin in presence of Au^{3+} or pre-generated AuNP follows similar degradation kinetics, which insists the detailed study of TiO_2 catalyst and its' modified materials while doing photolysis. The filtrates, superannuated solutions and residues characterized by different techniques under the study are discussed below.

The changes in colors of the solutions and the residues on membrane filters from orange to dark purple (Figure 2b) revealed the degradation of eosin as well as the formation of AuNP. The size of AuNP produced during the study was $\sim 100 \text{ nm}$ as determined in DLS experiments with superannuated AuNP samples (wherein TiO_2 was removed through centrifuge).

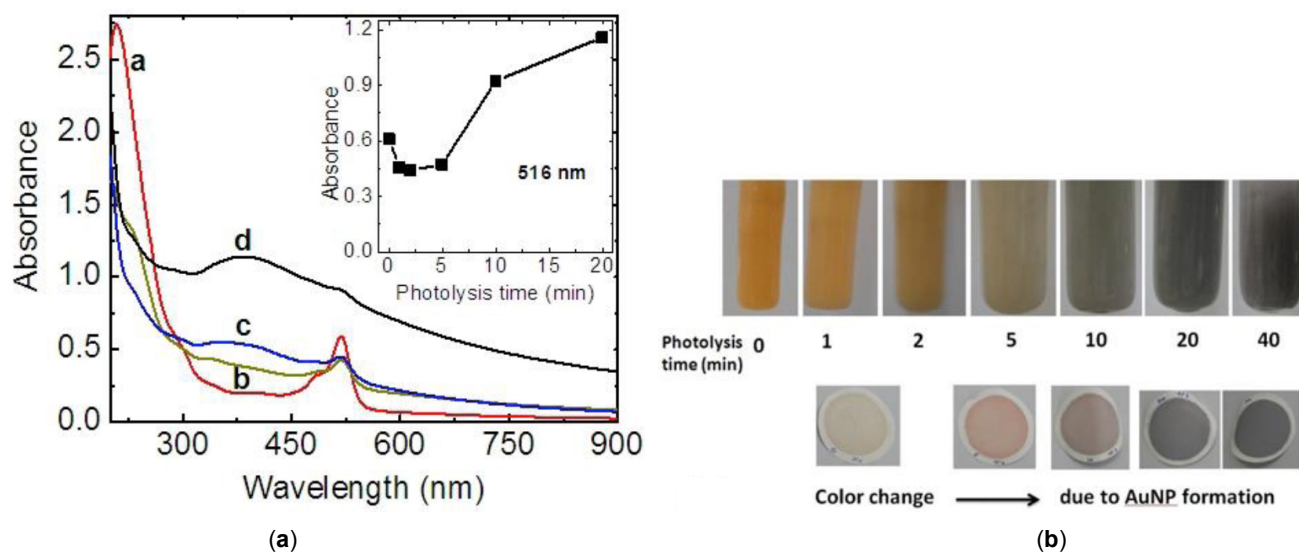


Figure 2: (a) UV-visible spectra of superannuated solutions a: before photolysis, b: 1 min; c: 2 min; d: 10 min after photolysis. Inset: the variation in absorbance at 516 nm vs photolysis time. (b) Photographs of the samples containing 0.1% (w/v) TiO_2 , $2 \times 10^{-4} \text{ M}$ eosin and $2 \times 10^{-4} \text{ M}$ Au^{3+} in aqueous systems before and after photoirradiation up to 40 min along with photographs of residues on membrane filters of before and after 5-40 min irradiated same samples.

Figure 3 shows the XRD patterns of the residue materials of TiO_2 , before and after 1 & 20 min photo-irradiated eosin- Au^{3+} - TiO_2 samples on membrane filters. The XRD spectra of TiO_2 (peaks at $2\theta = 25^\circ$ & 48°) were identical to that of the anatase TiO_2 [13, 14]. It is also noticed from Figure 3 that, the XRD patterns of TiO_2 remained unaffected in eosin- TiO_2 systems containing Au^{3+} . However, for 1 and 20 min photo-irradiated eosin- TiO_2 - Au^{3+} samples, the considerable change in peaks intensities at 2θ 38° and 62° (see Figure 3) is due to AuNP formation [14, 15]. It is important to note that with formation of AuNP the spectral peaks tends to be broader and the broadness increases with increase in AuNP concentrations [16, 17]. The peak intensity at $2\theta = 25^\circ$ and 38° decreased considerably (spectrum c Figure 3) when the samples were photo-irradiated for 1 min. This was decreased drastically (spectrum d Figure 3) when samples were photo-irradiated further to 20 min, hinting the incorporation of AuNP onto TiO_2 .

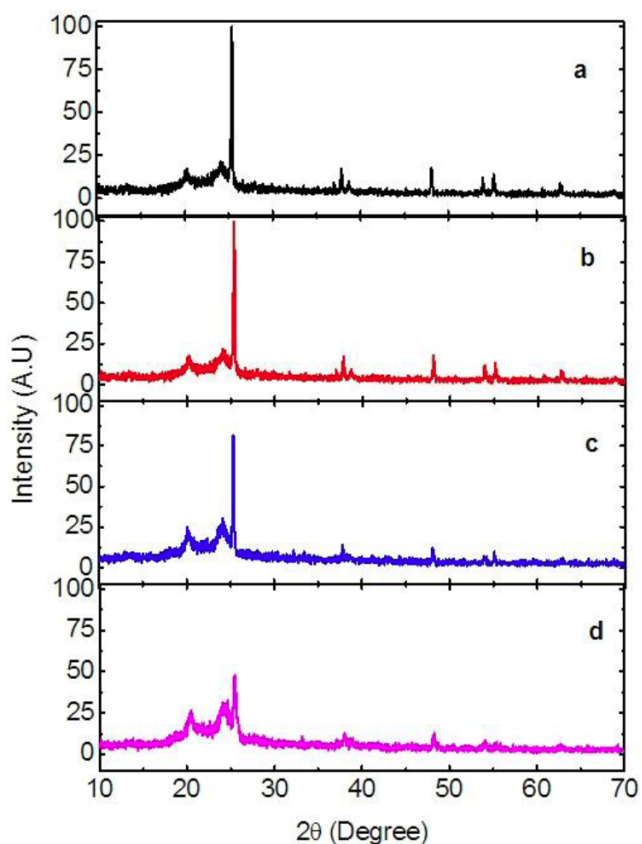


Figure 3: XRD patterns of residues on membrane filters **a:** 0.1% (w/v) TiO_2 ; **b:** 0.1% (w/v) TiO_2 , 2×10^{-4} M eosin and 2×10^{-4} M Au^{3+} ; and **c:** 1 min and **d:** 20 min photoirradiated samples of 0.1% (w/v) TiO_2 , 2×10^{-4} M eosin and 2×10^{-4} M Au^{3+} in aqueous systems.

Similarly the Raman scattering spectra recorded for all these above samples (residues on membrane filters)

are shown in Figure 4. The background membrane filter (Raman spectrum not shown) did not show any active peak within 200 - 1000 cm^{-1} spectral region. Moreover, in presence of TiO_2 (Figure 4 spectrum 'a') three distinct peaks were observed below 1000 cm^{-1} region (640 , 517 and 397.6 cm^{-1}), which are quite similar to previous report [18]. The presence of eosin and Au^{3+} ions did not lead to any significant change in spectral properties of TiO_2 (spectrum 'b') within 1000 cm^{-1} region except there is decrease in peaks intensities. Moreover, in presence of two different concentrations of AuNP (produced due to photo-irradiation for 1 & 20 min), the peaks de-shaping (broadening, and blue shifting to 630 , 510 and 394 cm^{-1}) within 1000 cm^{-1} were observed, which is due to the active interaction between TiO_2 and AuNP (spectra c & d) that changed the vibration & structural properties of TiO_2 [18]. The high content of AuNP in 20 min photo-irradiated sample was exhibited significant peak shifting & broadening in contrast to 1 min photolysis sample.

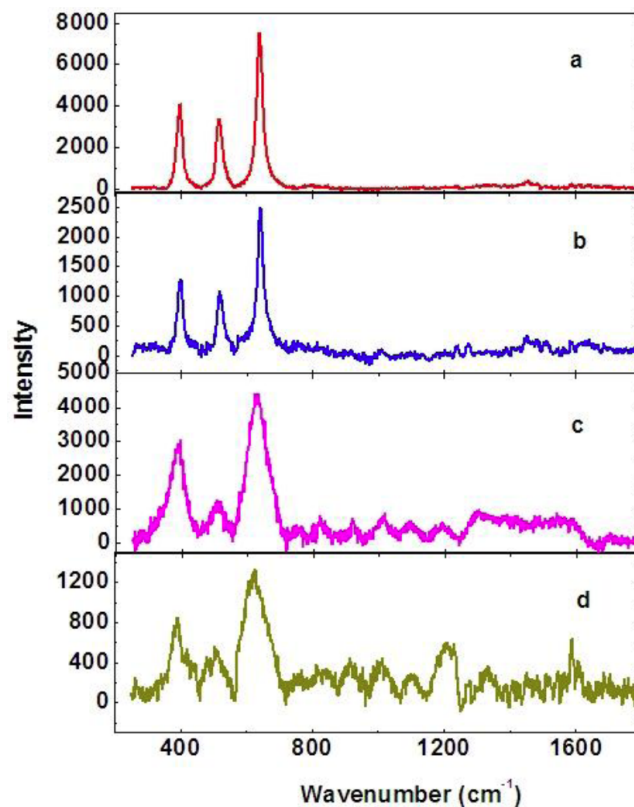


Figure 4: Raman shift spectra recorded for residues of different samples on membrane filter **a:** 0.1% (w/v) TiO_2 ; **b:** 0.1% (w/v) TiO_2 , 2×10^{-4} M eosin and 2×10^{-4} M Au^{3+} ; **c:** after 1 min and **d:** after 20 min photolysis on 0.1% (w/v) TiO_2 , 2×10^{-4} M eosin and 2×10^{-4} M Au^{3+} .

SEM images (Figure 5a) exhibit larger size (~ 100 nm) and morphological change (coagulated) in TiO_2

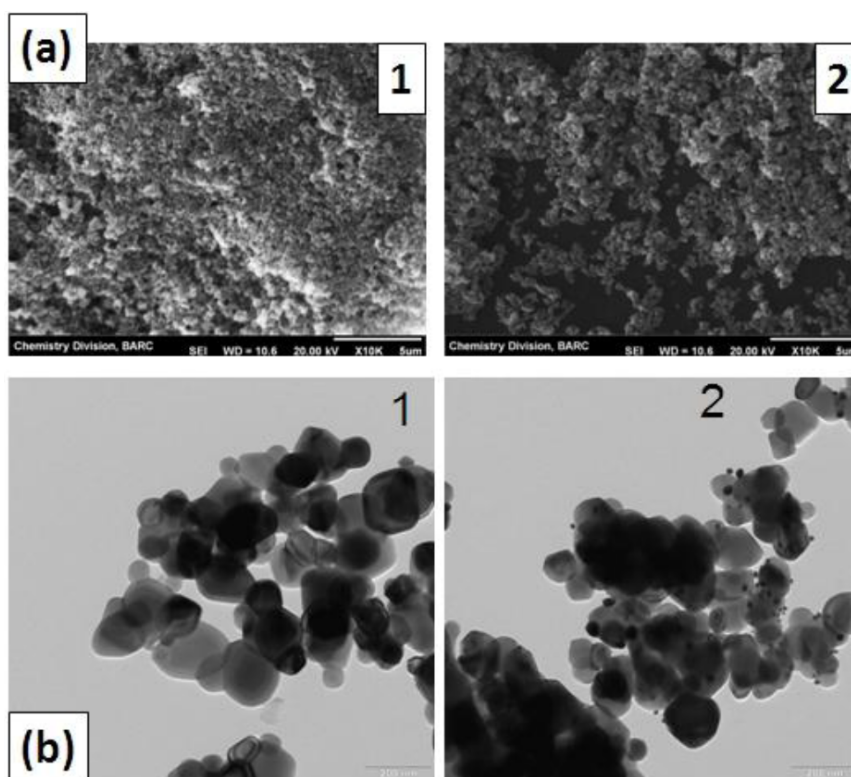


Figure 5: SEM (a) & TEM (b) images of TiO₂ (1) and Au/TiO₂ (2)

AuNP materials (Figure 5a image 2) than in the plain TiO₂ (Figure 5a image 1). Furthermore, in Figure 5b image 2, the TEM image obtained with 20 min photo-irradiated 0.1% (w/v) TiO₂, 2x10⁻⁴ M eosin and 2x10⁻⁴ M Au³⁺ sample exhibited AuNP (~60 nm) incorporated on TiO₂ surfaces that probably revealed high mineralization efficiency in contrast to only TiO₂ (Figure 5b image 1).

It was understood from the materials studies (UV-Vis spectral measurement where 300-450 nm broad band along with the absorbance change at 520 nm, significant decrease in peak intensity at 2θ 25° in XRD pattern, TEM image and Raman peaks shifting & broadening) that the difference in morphological change of TiO₂ due to eosin photolysis in water with suspended TiO₂ in presence Au³⁺ lead to the formation of in-situ AuNP and/or Au-doped TiO₂.

3.5. Eosin-OH/ N₃· Reaction Intermediates

To understand the eosin oxidative degradation mechanism through hole (considered as ·OH [19, 20]) initiative reactions, the pulse radiolysis studies were revisited on the reactions of eosin with ·OH/N₃· radicals at pH 6.8. The experimental set up for pulse radiolysis study in this institute has been reported elsewhere [21] in which 7 MeV electron beam of 200 ns pulse duration

(dose rate 20 Gy per pulse determined as described elsewhere [22]) was used for sample irradiation. In water/aqueous medium, the primary species generated due to interaction of high-energy radiation (electron beam in the present case) in pico second time and diffused homogeneously throughout the medium within 0.1 μs time are e_{aq}⁻, H·, ·OH, H₂, H₂O₂, H₃O⁺ [5]. Amongst these, e_{aq}⁻ and H· are reducing radicals and ·OH is oxidizing radical. At high pH (pH ≥ 10) using N₂O-purged systems, the primary radiolytic species viz. e_{aq}⁻, H· (H + H₂O ⇌ e_{aq}⁻ + H₃O⁺ pK_a = 9.6 [5]) and ·OH remain as total ·OH through N₂O + e_{aq}⁻ → N₂ + OH⁻ + ·OH reaction. Furthermore, in presence of oxygen, ·H and e_{aq}⁻ form less reactive species HO₂· through (O₂ + ·H → HO₂·) and O₂⁻ (O₂ + e_{aq}⁻ → O₂⁻) reactions [23], allowing the radiolytically generated ·OH in the system to interact with solute available (eosin in this case). In presence of NaN₃ under identical conditions, N₃· was generated through N₃⁻ + ·OH → N₃· + OH⁻ [23]. The selection of ·OH and N₃· under the study was made because of their different reaction nature, former undergoes both addition and electron transfer reactions while the later reacts mainly through electron transfer type mechanism. The reactions of ·OH and N₃· with eosin studied separately are discussed below.

The spectrum 'a' in Figure 6 shows the transient absorption spectrum obtained in eosin-OH reaction at

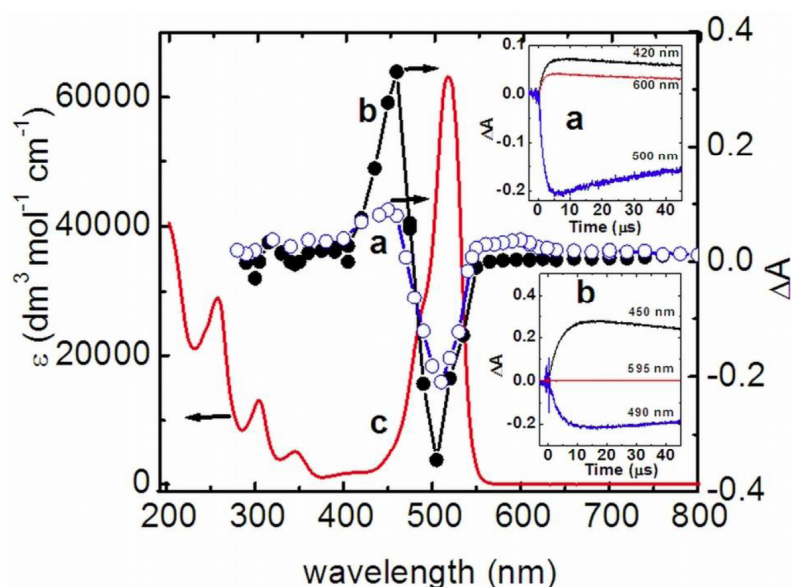


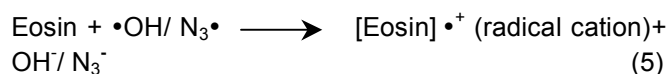
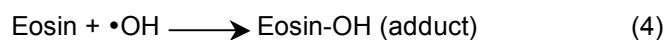
Figure 6: The transient absorption spectra of a: eosin-OH and b: eosin-N₃ reactions species at pH 6.8 along with c: UV-Vis spectrum of 5x10⁻⁵ M eosin in water. Insets: a: the time profiles obtained at 420, 500 and 600 nm in eosin-OH reaction and b: the time profiles obtained at 450, 490 and 595 nm in eosin-N₃ reaction under identical conditions.

pH 6.8. This spectrum exhibits two peaks with absorption maxima around 450 and 600 nm and a strong bleaching at 510 nm. The observed transient spectrum is quite similar to the reported spectrum [24, 25]. The rate for ·OH reaction with eosin was determined from the formation of the transient intermediates absorption at 450 and 600 nm adopting the pseudo first order reaction rate determination concept. The reaction rates were evaluated to be 1.4x10¹⁰ M⁻¹ s⁻¹ (close to the reported value [25]) and 5.4x10⁹ M⁻¹ s⁻¹ respectively using transient growth profiles obtained at 640 and 450 nm. The time profiles at 600 and 420 nm (inset 'a' in Figure 6) with different kinetics demonstrate that the 400 and 600 nm species are different. It is important to note that the contribution due to ·H in eosin-OH reaction intermediate species was verified in pulse irradiated N₂O-purged 5x10⁻⁵ M eosin in aqueous solutions containing 1 M tertiary butanol (an ·OH scavenger) [23] experiments at pH 6.8. The negligible signals both at 450 and 600 nm regions under the study reveals insignificant contribution of ·H in above-discussed eosin-OH reaction.

Similarly, the spectrum 'b' in Figure 6 depicts the transient absorption spectrum recorded during eosin-N₃ reaction. This spectrum exhibits only one peak with absorption maximum at 450 nm along with a strong bleaching at 510 nm. The reaction rate for N₃ reaction with eosin determined from the formation time profiles of transient intermediates absorption at 450 nm was found to be 3.0x10⁹ M⁻¹ s⁻¹, which is close to ·OH

reaction with eosin evaluated using 450 nm time profiles.

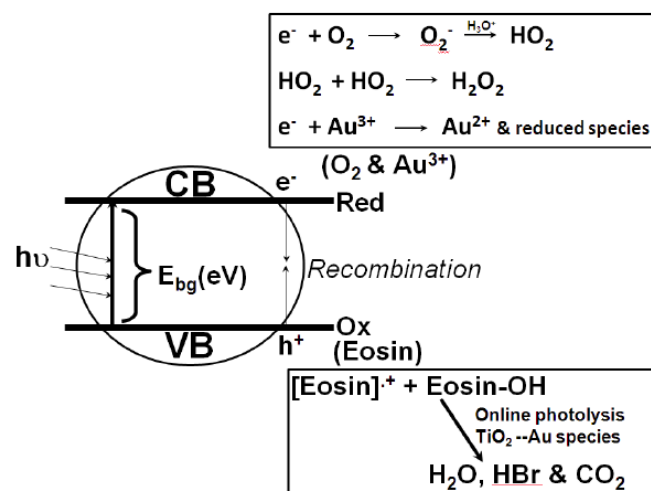
On comparison of spectra a & b in Figure 6 it was observed that in ·OH reaction there were two different intermediates: one is responsible for the absorption around 400 nm and other possesses absorption in 600 nm region. In N₃ reaction the absence of 600 nm absorbing species reveals that the formation of 600 nm absorbing species was exclusively due to ·OH addition and/or its subsequent reaction intermediates originated from eosin-OH adduct species. The percentage of two different species generated in ·OH reactions with eosin was evaluated to be 25% radical cation (450 nm absorbing species) and 75% ·OH adduct species (600 nm absorbing species). This was evaluated based on the comparison of the absorbance values obtained from equal quantity of radicals (·OH/N₃) generated in two different systems (*G*-values for ·OH/N₃ = 5.5 [5] at identical conditions. The possible reactions are:



The following interpretations are therefore made: in presence of TiO₂ the mineralization of eosin was more as compared to only eosin systems where photo color-fading took place to a lesser extent as breaking of some weak chromophoric bonds occurred. The mineralization in aerated TiO₂ systems was more

because the oxygen presence in the system holds dual role: i) as an electron scavenger: a part of photogenerated e^- was scavenged by O_2 (preventing recombination reaction (backward reaction 1) resulting more hole available for oxidation of eosin. ii) Secondly, the generated eosin-hole/OH reaction intermediate species react with available oxygen undergoing subsequent mineralization through oxy/hydroxy intermediates. It is noteworthy to include at this juncture that the radical cations in general are less/negligible reactive to oxygen [26]. Hence, the eosin-OH adduct and/or its' associated intermediates are responsible for eosin mineralization.

In aerated Au^{3+} and TiO_2 systems, Au^{3+} was demonstrated as a better electron scavenger than oxygen resulting enhanced eosin mineralization. The different concentrations of Au^{3+} exhibited different mineralization kinetics revealing the mineralization in presence of air was Au^{3+} concentration dependent. The important issue under the study is the formation of AuNP (following reduction reactions) even in presence of air (~20% O_2 equivalent to 0.24 mM), which confirms Au^{3+} a better electron scavenger than O_2 with respect to high rate of eosin mineralization. Moreover, as reported earlier, in the gold capped TiO_2 i.e. Au/ TiO_2 system the metal nanoparticles has been considered as an electron sink/trapper [10, 14, 27, 28], where the electrons in the conduction band can migrate towards the Au surface, thereby preventing the recombination of e^- and h^+ pairs. This transferred electron in Au surface was consumed by oxygen available therein on the surface forming superoxide radical anion (O_2^-), and subsequently converted into $\cdot OH$ via HO_2/H_2O_2 formation, resulting enhanced eosin mineralization. Nevertheless, in metal ions containing systems, after formation of metal nanoparticles (as soon as AuNP color appears) the systems behave both as metal doped as well as metal ions containing systems, wherein both metal ions and its nanoparticles play significant role in eosin mineralization. This happens only when the photolysis was kept on, because after photolysis (photolight off condition) the colors of nanoparticles remained steady, indicating the negligible contribution of eosin mineralization due to thermal reaction of the nanoparticles with eosin. It is noteworthy to include that the active role of various intermediates starting from reduced metal ions/metal atom to oligomers/small aggregates of sub-nano- or nano-sized gold metal particles was significant in eosin mineralization. The possible photo-catalytic reactions taking place during mineralization of eosin are shown in Scheme 2.



Scheme 2: Schematic of Eosin mineralization.

CONCLUSION

Enhanced mineralization of eosin has been demonstrated under the study in presence of both Au(III) ions and its' in situ generated AuNP in oxygen containing systems. The strong interaction of AuNP with TiO_2 photo-catalyst was observed in Raman shifting during material characterization. The reaction intermediates both eosin-OH/hole adduct as well as radical cation (differentiated in pulse radiolysis studies) were generated initially in mineralization process, wherein eosin-OH/hole adduct is probably undergoing mineralization in presence of oxygen on photo-irradiation. In presence of Au^{3+} ($0.2-2 \times 10^{-4}$ M), the eosin mineralization was faster ($0.180 - 0.274 \text{ min}^{-1}$) as compared to sole TiO_2 systems (0.004 min^{-1}), which is due to the contribution of Au^{3+} and the in situ generated AuNP in organics degradation process. This finding not only contributes in updating the eosin mineralization method, but this methodology also evolves as a convenient technique for their utilization in pollution control.

ACKNOWLEDGEMENTS

This research was carried out under the Plan Sub-project XII-N-R&D-02.1. The author thanks Department of Atomic Energy, Government of India and Bhabha Atomic Research Centre for the funding. P.S. thanks Sri Guru Granth Sahib World University and BARC authorities for approving his summer intern ship. The authors thank Mr. A. Das for Raman spectra.

REFERENCES

- [1] Eosin as carcinogen: <http://www.ihcworld.com/royellis/ABCSafe/chemicals/eosin-y.htm> accessed on 24 June 2016

- [2] Eosin hazard: <http://cameochemicals.noaa.gov/chemicals/20332> accessed on 24 June 2016
- [3] Bahenmann DW. *in* Pelizzetti E, Schiavello M, Eds. Photochemical conversion and storage of solar energy, Kluwer, Dordrecht 1991; p. 251.
- [4] Hoffmann MR, Martin ST, Choi W, Bahenmann DW. Applications of semiconductor photocatalysis. *Chem Rev* 1995; 95: 69-96. <https://doi.org/10.1021/cr00033a004>
- [5] Spinks JWT, Woods RJ, Eds. *An Introduction to Radiation Chemistry*, 3rd edn., Wiley, New York 1990.
- [6] Tabata Y, Ed. *Pulse Radiolysis*, CRC Press, Boca Raton 1991.
- [7] Yin M, Li Z, Kou J, Zou Z. Mechanism Investigation of Visible light-Induced Degradation in a Heterogeneous TiO₂/Eosin Y/Rhodamine B System. *Environ Sci Technol* 2009; 43: 8361-8366. <https://doi.org/10.1021/es902011h>
- [8] Zhang F, Zhao J, Shen T, Hidaka H, Pelizzetti E, Serpone N. TiO₂-assisted photodegradation of dye pollutants II. Adsorption and degradation kinetics of eosin in TiO₂ dispersions under visible light irradiation. *Appl Catal B Environ* 1998; 15: 147-156. [https://doi.org/10.1016/S0926-3373\(97\)00043-X](https://doi.org/10.1016/S0926-3373(97)00043-X)
- [9] Ayati A, Ahmadpour A, Bamoharram FF, Tanhaei B, Mänttari M, Sillanpää M. A review on catalytic applications of Au/TiO₂ nanoparticles in the removal of water pollutant. *Chemosphere* 2014; 107: 163-174. <https://doi.org/10.1016/j.chemosphere.2014.01.040>
- [10] Padikkaparambil S, Narayanan B, Yaakob Z, Viswanathan S, Tasirin SM. Au/TiO₂ reusable photocatalysts for dye degradation. *Internat. J Photoener* 2013; Article ID 752605, 10 pages.
- [11] Dey GR, Belapurkar AD, Kishore K. Photoreduction of carbon dioxide to methane using TiO₂ as suspension in water. *J Photochem Photobiol A Chem* 2004; 163: 503-508. <https://doi.org/10.1016/j.jphotochem.2004.01.022>
- [12] Liang H. Study on the Effects of the Preparation Conditions on the Combination of Eosin Dye and TiO₂. *Appl Mech Mater* 2014; 526: 86-90. <https://doi.org/10.4028/www.scientific.net/AMM.526.86>
- [13] Li B, Wang X, Yan M, Li L. Preparation and characterization of nano-TiO₂ powder. *Mater Chem Phys* 2002; 78: 184-188. [https://doi.org/10.1016/S0254-0584\(02\)00226-2](https://doi.org/10.1016/S0254-0584(02)00226-2)
- [14] Gao Y, Fan X-B, Zhang W-F, Zhao Q-S, Zhang G-L, Zhang F-B, Li Y. Enhanced photocatalytic degradation of methyl orange by Au/TiO₂ nanotubes. *Mater Lett* 2014; 130: 1-4. <https://doi.org/10.1016/j.matlet.2014.05.076>
- [15] Doremus RH. Optical Properties of Small Gold Particles. *J Chem Phys* 1964; 40: 2389-2396. <https://doi.org/10.1063/1.1725519>
- [16] Belapurkar AD, Kamble VS, Dey GR. Photooxidation of ethylene in gas phase and methanol and formic acid in liquid phase on synthesized TiO₂ and Au/TiO₂ catalysts. *Mater Chem Phys* 2010; 123: 801-805. <https://doi.org/10.1016/j.matchemphys.2010.05.063>
- [17] Dey GR. Effects of metal ions on H₂ generation during photolysis of suspended TiO₂ in aqueous systems under different ambient conditions. *J Appl Sol Chem Model* 2015; 4: 63-71. <https://doi.org/10.6000/1929-5030.2015.04.01.5>
- [18] Choi HC, Jung YM, Kim SB. Size effects in the Raman spectra of TiO₂ nanoparticles. *Vib Spec* 2005; 37: 33-38. <https://doi.org/10.1016/j.vibspec.2004.05.006>
- [19] Kamat PV. Photochemistry on Nonreactive and Reactive (Semiconductor) Surface. *Chem Rev* 1993; 93: 267-300. <https://doi.org/10.1021/cr00017a013>
- [20] Dey GR. Significant roles of oxygen and unbound ·OH radical in phenol formation during photocatalytic degradation of benzene on TiO₂ suspension in aqueous system. *Res Chem Intermed* 2009; 35: 573-587. <https://doi.org/10.1007/s11164-009-0066-0>
- [21] Guha SN, Moorthy PN, Kishore K, Naik, DB, Rao KN. One electron reduction of thionine studied by pulse radiolysis. *Proc Indian Acad Sci (Chem Sci)* 1987; 99: 261-271.
- [22] Buxton GV, Stuart CR. Re-evaluation of the thiocyanate dosimeter for pulse radiolysis. *J Chem Soc Faraday Trans.* 1995; 91: 279-281. <https://doi.org/10.1039/ft9959100279>
- [23] Buxton GV, Greenstock CL, Helman WP, Ross AB. Critical review of rate constants for reactions of hydrated electron, hydrogen atoms and hydroxyl radicals (OH/O⁻) in aqueous solution. *J Phys Chem Ref Data* 1988; 17: 513-886. <https://doi.org/10.1063/1.555805>
- [24] Grossweiner LI, Rodde AF, Sandberg JG, Chrysochoos J. Pulse Radiolysis of Aqueous Eosin. *Nature* 1966; 210: 1154-1156. <https://doi.org/10.1038/2101154a0>
- [25] Chrysochoos J, Ovidia J, Grossweiner LI. Pulse Radiolysis of Aqueous Eosin. *J Phys Chem* 1967; 71: 1629-1636. <https://doi.org/10.1021/j100865a014>
- [26] Dey GR, Hermann R, Naumov S, Brede O. Encounter geometry determines product characteristics of electron transfer from 4-hydroxythiophenol to n-butyl chloride radical cations. *Chem Phys Let* 1999; 310:137-144. and reference therein.
- [27] Subramanian V, Wolf EE, Kamat PV. Effect of metal particle size on the fermi level equilibration. *J Am Chem Soc* 2004; 126: 4943-4950. <https://doi.org/10.1021/ja0315199>
- [28] Kamat PV. Photoinduced transformations in semiconductor-metal nanocomposite assemblies. *Pure Appl Chem* 2002; 74: 1693-1706. <https://doi.org/10.1351/pac200274091693>